

Morphological changes in human gastric epithelial cells induced by nuclear targeting of *Helicobacter pylori* urease subunit A[§]

Jung Hwa Lee¹, So Hyun Jun¹, Jung-Min Kim²,
Seung Chul Baik^{2*}, and Je Chul Lee^{1*}

¹Department of Microbiology, Kyungpook National University School of Medicine, Daegu 700-422, Republic of Korea

²Department of Microbiology, Gyeongsang National University School of Medicine, Gyeongsang Institute of Health Science, Jinju 660-701, Republic of Korea

(Received Feb 12, 2015 / Revised May 14, 2015 / Accepted May 15, 2015)

Nuclear targeting of bacterial proteins and their pathological effects on host cells are an emerging pathogenic mechanism in bacteria. We have previously reported that urease subunit A (UreA) of *Helicobacter pylori* targets the nuclei of COS-7 cells through nuclear localization signals (NLSs). This study further investigated whether UreA of *H. pylori* targets the nuclei of gastric epithelial cells and then induces molecular and cellular changes in the host cells. *H. pylori* 26695 strain produced and secreted outer membrane vesicles (OMVs). UreA was translocated into gastric epithelial AGS cells through outer membrane vesicles (OMVs) and then targeted the nuclei of AGS cells. Nuclear targeting of rUreA did not induce host cell death, but resulted in morphological changes, such as cellular elongation, in AGS cells. In contrast, AGS cells treated with rUreAΔNLS proteins did not show this morphological change. Next generation sequencing revealed that nuclear targeting of UreA differentially regulated 102 morphogenesis-related genes, of which 67 and 35 were up-regulated and down-regulated, respectively. Our results suggest that nuclear targeting of *H. pylori* UreA induces both molecular and cellular changes in gastric epithelial cells.

Keywords: nuclear targeting protein, urease, pathogenesis, outer membrane vesicles

Introduction

Helicobacter pylori colonizes or infects the gastric mucosa of more than half of the world's population, affecting as much as 90% of the population in countries with poor sanitation. *H. pylori* infection is known to be associated with the development of gastritis, peptic ulcers, chronic atrophy, and gastric adenocarcinoma (Suerbaum and Michetti, 2002; Yu

et al., 2011; Makobongo *et al.*, 2014; Seo *et al.*, 2014). However, the molecular mechanisms by which *H. pylori* contributes to the development of gastric diseases remain to be elucidated. Several virulence-associated determinants have been found to be associated with the pathogenesis of *H. pylori* and progression of gastric diseases. These include membrane-associated adhesins (blood-group-antigen-binding adhesin [BabA], sialic acid binding adhesin [SabA], adherence-associated lipoprotein A and B [AlpA/B], and outer inflammatory protein A [OipA]) (Ilver *et al.*, 1998; Yamaoka *et al.*, 2000; Mahdavi *et al.*, 2002; Odenbreit *et al.*, 2002), cytotoxin-associated gene A (CagA) (Handa *et al.*, 2007; Backert *et al.*, 2011; Wessler *et al.*, 2011), vacuolating cytotoxin A (VacA) (Cover and Blanke, 2005; Rassow, 2011), high temperature requirement A (HtrA) (Hoy *et al.*, 2010), peptidoglycan (Viala *et al.*, 2004), and γ -glutamyl transpeptidase (Kim *et al.*, 2007).

Nuclear targeting of bacterial proteins is a recently recognized pathogenic mechanism of bacteria that has a significant impact on host cell biology. Several bacteria, *Acinetobacter baumannii* (Choi *et al.*, 2008), *Chlamydia trachomatis* (Pennini *et al.*, 2010), *Klebsiella pneumoniae* (Lee *et al.*, 2009), *Salmonella enterica* (Haraga and Miller, 2003), *Shigella* species (Okuda *et al.*, 2005), and *Yersinia* species (Benabdillah *et al.*, 2004), are known to possess nuclear targeting proteins in eukaryotic cells. After translocation to the nuclei of host cells through nuclear localization signals (NLSs) (Lange *et al.*, 2007), bacterial proteins may directly or indirectly bind to the nuclear molecules of the host cells and then alter cell function or induce pathological changes in cells. Using bioinformatic analysis, we recently found that 49 functional or hypothetical *H. pylori* proteins carried putative NLSs in their amino acid sequences and, among these, 26 were experimentally shown to target the nuclei of COS-7 cells (Lee *et al.*, 2012). For instance, urease subunit A (UreA) could target the nuclei of COS-7 cells via a monopartite NLS, ₂₁KKRKEK₂₆. These results suggested that nuclear targeting of UreA may alter the biology of gastric epithelial cells if UreA is translocated from *H. pylori* to gastric epithelial cells during *in vivo* infection.

H. pylori produces a large quantity of urease, which accounts for 10–15% of the bacterial proteins (Hu and Mobley, 1990). *H. pylori* urease is a 1.1 MDa spherical assembly of 12 catalytic units, consisting of a monomer with two subunits, UreA (26.5 kDa) and UreB (60.3 kDa) (Ha *et al.*, 2001; Ge *et al.*, 2013). Urease is an intracellular enzyme that catalyzes the hydrolysis of urea to form ammonia and carbon dioxide. Urease production is essential to the survival of *H. pylori* under the acidic conditions encountered during colonization or infection in the stomach (Eaton and Krakowka,

*For correspondence. (S. C. Baik) E-mail: sbaik@gnu.ac.kr; Tel.: +82-55-772-8084; Fax: +82-55-772-8089 / (J. C. Lee) E-mail: leejc@knu.ac.kr; Tel.: +82-53-420-4844; Fax: +82-53-427-5664

[§]Supplemental material for this article may be found at <http://www.springerlink.com/content/120956>.

1994; Dunn *et al.*, 1997). The main role of the urease produced by *H. pylori* is thought to be neutralization of the acidic microenvironment by production of ammonia. Urease also displays biological effects that are independent of its enzymatic activity, such as inducing the production of pro-inflammatory cytokines (Harris *et al.*, 1996), transendothelial migration of T cells (Enarsson *et al.*, 2005), and expression of inducible nitric oxide synthesizing enzyme (Gobert *et al.*, 2002), which mediates tissue inflammation and injury. Upon bacterial autolysis, intrabacterial urease is released and binds to the extracellular surface of viable *H. pylori*, where it represents about 30% of the total cell urease content (Dunn *et al.*, 1997). Furthermore, outer membrane vesicles (OMVs) secreted from *H. pylori* contain structural and accessory proteins of urease, including UreA, UreB, UreF, and UreH (Olofsson *et al.*, 2010). Given this background, we hypothesized that OMVs deliver intrabacterial and surface-bound urease of *H. pylori* to gastric epithelial cells, which can then induce alteration of host cell biology. This study investigated the translocation of UreA from *H. pylori* to host cells via OMVs and the subsequent molecular and cellular changes in gastric epithelial cells induced by nuclear targeting of UreA.

Materials and Methods

Bacterial strains and cell culture

H. pylori 26695 strain was obtained from the *H. pylori* Korean Type Culture Collection (Gyeongsang National University School of Medicine, Jinju, Korea). *Escherichia coli* DH5 α and *E. coli* BL21 (DE3) were used for DNA cloning and production of recombinant UreA (rUreA) proteins, respectively. *H. pylori* was grown on Brucella agar medium (Difco) supplemented with 10% fetal bovine serum (FBS; HyClone) at 37°C in 10% CO₂. *E. coli* strains were grown in Luria-Bertani (LB; Difco) broth at 37°C. AGS cells, originally derived from human gastric carcinoma tissue, were obtained from the Korean Cell Line Bank. AGS cells were grown in RPMI 1640 medium (HyClone) supplemented with 10% FBS, 100 U/ml penicillin, and 20 μ g/ml streptomycin under a humidified atmosphere containing 5% CO₂. AGS cells were seeded in 6- or 12-well tissue culture plates for the transfection of plasmids or direct delivery of recombinant proteins.

Gateway recombinational cloning of *ureA*

Genomic DNA was purified from *H. pylori* 26695 using a SolGent™ Genomic DNA Prep kit (SolGent) and was then used as a template for polymerase chain reaction (PCR). PCR was performed using 1.5 U Platinum Pfx DNA polymerase (Invitrogen), 2 μ l of 10 \times Pfx amplification buffer, 0.3 mM dNTP mixture, 1 mM MgSO₄, 10 pM of each primer, and template DNA (100 ng). PCR reactions were performed in two steps: The first step of PCR, employing *ureA*-specific primers (5'-ACA AAA AAG CAG GCT CCA CCA TGA AAC TCA CCC CAA AAG AGT T-3' and 5'-ACA AGA AAG CTG GGT TCT CCT TAA TTG TTT TTA CAT AGT TG-3'; underlined nucleotides indicate *attB1* and *attB2* adapter sequences, respectively), was conducted as

follows: one cycle of 95°C for 3 min; 30 cycles each consisting of 95°C for 30 sec, 55°C for 30 sec, and 72°C for 2 min; and a final elongation step at 72°C for 10 min. The PCR products so obtained were then used as a template in the second step of PCR, which employed the adapter primers for *attB1* (5'-GGG GAC AAG TTT GTA CAA AAA AGC AGG CT-3') and *attB2* (5'-GGG GAC CAC TTT GTA CAA GAA AGC TGG GT-3'); this generated the full-length *attB1* and *attB2* sites flanking *ureA* of *H. pylori*. The amplified *ureA* was recombined into the pDONR207 vector (Invitrogen) by using BP reactions. The plasmid pDONR207 was mixed with 2 μ l of each *attB*-linked PCR product in 15 μ l of BP reaction mixture containing 3 μ l BP clonase I enzyme mix (Invitrogen). After incubation at 25°C for 60 min, proteinase K was added and then each reaction was incubated at 37°C for 10 min. BP reaction mixtures were used directly for bacterial transformation. Aliquots of the entry clone were used for transformation of *E. coli* DH5 α cells, and bacteria were plated on LB medium containing 50 μ g/ml of gentamicin. A single colony subsequently obtained from these plates was tested by colony-PCR with specific primers for *ureA* and the amplicon was sequenced using an ABI Prism 3730XL Analyzer (Applied Biosystems). The entry clone specific for *ureA* was then used for the generation of green fluorescent protein (GFP)-tagged clones or production of recombinant proteins in a reaction mixture containing 2 μ l LR clonase II enzyme mix (Invitrogen), 150 ng pcDNA™6.2/N-EmGFP-DEST vector (Invitrogen) for GFP-tagged clones or pET160-DEST (Invitrogen) for the production of recombinant proteins. After incubation at 25°C for 3 h, proteinase K was added and each reaction mixture was further incubated at 37°C for 10 min. The LR reactions were used to transform *E. coli* DH5 α , as described above. Transformants were selected on LB plates containing 50 μ g/ml ampicillin.

Transfection of the constructed plasmids in AGS cells

The plasmid constructs obtained from LR reactions were extracted using an Exprep™ plasmid SV kit (GeneAll), and plasmid DNA was diluted in 100 μ l of Opti-MEM MEM® I medium (Invitrogen). Plasmid DNA (1.6 μ g) was incubated with 4 μ l Lipofectamine™ 2000 (Invitrogen), diluted in 96 μ l of Opti-MEM MEM® I medium, for 45 min at room temperature and this mixture was subsequently added to the cells.

Production of rUreA proteins and direct delivery of recombinant proteins into AGS cells

The plasmid constructs of *ureA* cloned into pET160-DEST using the Gateway cloning system were transformed into *E. coli* BL21 (DE3) and recombinant proteins were overexpressed after induction with 1 mM of isopropyl β -D-1-thiogalactopyranoside at 37°C for 4 h. Recombinant proteins were purified using a nickel-column (Amersham Biosciences) and lipopolysaccharide (LPS) was removed by polymyxin B-coated beads (Sigma-Aldrich). The protein concentration was determined using a modified BCA assay (Thermo Scientific). Concentrations of LPS were determined using a *Limulus* Amebocyte lysate test kit (Sigma-Aldrich), and the quantity of LPS in the recombinant proteins was found to be \leq 0.01

ng/mg. His-tagged recombinant UreA proteins were delivered directly into AGS cells using a Pro-Ject™ Protein Transfection Reagent kit (Pierce) according to the manufacturer's instructions. This system is a unique cationic lipid-based carrier system for the delivery of biologically active proteins into living cells.

Isolation of OMVs

The OMVs produced by *H. pylori* were prepared as described previously (Kwon *et al.*, 2009). Briefly, *H. pylori* 26695 strain was grown in Brucella broth (Difco) supplemented with 10% horse serum in a 90-mm diameter petri dish to the early stationary phase under the following conditions: 10% CO₂, 100% humidity, and a temperature of 37°C (Joo *et al.*, 2010). Bacterial cells were removed by centrifugation at 6,000 × g for 20 min at 4°C. The supernatants were filtered with a QuixStand Benchtop System (GE Healthcare) by using a 0.2 μm-sized hollow fiber membrane (GE Healthcare) and concentrated with a QuixStand Benchtop System using a 100 kDa hollow fiber membrane (GE Healthcare). The concentrated bacterial supernatant containing OMVs was ultracentrifuged at 150,000 × g for 3 h at 4°C. The pellets were resuspended in 1.25 ml of phosphate-buffered saline (PBS) and layered over a sucrose gradient (1.25 ml each of 2.5, 1.6, and 0.6 M sucrose). The samples were centrifuged at 200,000 × g for 20 h at 4°C, and four fractions of equal volumes were collected from the bottom. Sucrose was removed by ultracentrifugation at 150,000 × g for 3 h at 4°C, and the purified OMVs were resuspended in PBS. The sucrose density and protein concentration were determined using refractometry and the Bradford assay (Bio-Rad Laboratories), respectively. The purified OMVs were checked for sterility and stored at -80°C until required for use.

Preparation of bacterial lysates and outer membrane proteins

After culturing of *H. pylori* 26695 strain in Brucella broth, bacterial cells were centrifuged at 6,000 × g for 20 min at 4°C and resuspended in sodium dodecyl sulfate-polyacrylamide gel electrophoresis (SDS-PAGE) loading buffer (1 M Tris-HCl; pH 6.8, 10% SDS, 1% bromophenol blue, glycerol, and β-mercaptoethanol). The samples were boiled for 10 min to prepare bacterial lysates. For the preparation of outer membrane proteins, bacterial cells were resuspended in 10 mM HEPES buffer containing 1 mM EDTA and 1 mM phenylmethylsulfonyl fluoride (Smiley *et al.*, 2013). The bacterial cells were disrupted by sonication (Branson Sonic S-450A). Unbroken cells were removed by centrifugation and bacterial lysates were resuspended in 10 ml of 10 mM HEPES and then DNase and RNase (Sigma-Aldrich) were added to a final concentration of 0.1 mg/ml for 2 h at 37°C. After ultracentrifugation at 100,000 × g for 1 h, the pellets were solubilized in 10 ml of 2% sarcosine (Sigma-Aldrich) and incubated for 30 min at room temperature. The samples were ultracentrifuged at 100,000 × g for 1 h and the outer membrane proteins were subsequently dissolved in PBS. The protein concentrations were determined using the Bradford assay (Bio-Rad Laboratories).

Subcellular fractionation of AGS cells and western blotting of UreA

AGS cells were transfected with the destination vector pcDNA™6.2/N-EmGFP-DEST and plasmid constructs of *ureA* in pcDNA™6.2/N-EmGFP-DEST, generated using the Gateway cloning system, and were then incubated at 37°C for 24 h. After harvesting the adherent cells, the nuclear and cytosolic fractions were isolated using a Nuclear/Cytosol fractionation kit (Bio-Vision) according to the manufacturer's instructions. The samples were separated by 12% SDS-PAGE, followed by electrotransfer onto nitrocellulose membranes (Hybond-ECL; GE Healthcare). The blots were blocked in 5% non-fat skim milk and incubated with a monoclonal anti-mouse UreA antibody. A monoclonal antibody against UreA was supplied by Department of Microbiology, Gyeongsang National University School of Medicine, Jinju, Korea (Kim *et al.*, 1991). UreA proteins were visualized by incubation with horseradish peroxidase-conjugated goat anti-mouse IgG antibody (Molecular Probes), followed by enhanced chemiluminescence (ECL plus; GE Healthcare), according to the manufacturer's instructions.

Fluorescence and confocal laser microscopy

AGS cells were seeded at a density of 4×10^5 on glass coverslips in 6-well plates for 24 h. rUreA proteins were delivered directly into AGS cells using a protein transfection system and cells were incubated at 37°C for 4 h. After permeabilization of cells with Triton X-100, UreA was labeled with a monoclonal anti-mouse UreA antibody, followed by incubation with an Alexa-568-conjugated goat anti-mouse IgG antibody (Molecular Probes). The nuclei of AGS cells were stained with 4', 6-diamidino-2-phenylindole dihydrochloride (DAPI) (Molecular Probes). AGS cells were treated with *H. pylori* OMVs for 4 h. After permeabilization with Triton X-100, UreA was labeled with a monoclonal anti-mouse UreA antibody, followed by staining with an Alexa-488-conjugated goat anti-mouse IgG antibody (Molecular Probes). Samples were analyzed using a Carl-Zeiss confocal laser microscope. For staining of F-actin and myosin in AGS cells that had been treated with rUreA, cells were labeled with Alexa Fluor-568 phalloidin (Molecular Probes) and anti-myosin antibody (Abcam), followed by Alexa-488-conjugated goat anti-mouse IgG antibody (Molecular Probes), respectively. Cells were observed using a fluorescence microscope (Nikon).

Determination of cell viability

The cytotoxicity of AGS cells transfected with rUreA proteins was measured using the Premix WST1 Cell Proliferation Assay system (TaKaRa). AGS cells were seeded at a concentration of 2.0×10^5 cells/ml in a 96-well microplate. Cells were transfected with various concentrations of rUreA proteins using a protein transfection system and cells were incubated at 37°C for 24 h. The growth of AGS cells was monitored at 450 nm for 3 h after treatment with WST1.

Next generation sequencing (NGS)

Total RNA was isolated from AGS cells transfected with the destination vector pcDNA™6.2/N-EmGFP-DEST or the

plasmid constructs of *ureA* in pcDNATM6.2/N-EmGFP-DEST, and was then treated with RNase-free DNase I (New England BioLabs) for 30 min at 37°C to remove residual DNA. DNase I-treated total RNA was purified using the RNeasy RNA Isolation kit (Qiagen) and the integrity and quality of these samples were measured with an Agilent Bioanalyzer 2100 (Agilent). The samples with an OD_{260/280} > 1.8, 28s/18s > 1.5, and RIN > 9.0 were selected for sequencing. Oligo (dT)-conjugated beads were used to isolate poly(A) mRNA. First-strand cDNA was synthesized using random hexamer primers and reverse transcriptase (Invitrogen). The second-strand cDNA was synthesized using RNase H (Invitrogen) and DNA polymerase I (New England BioLabs). cDNA libraries were then prepared according to the manufacturer's instructions (Illumina). In total, we constructed one single-end cDNA library for each of two samples and sequenced these cDNA clones using the Illumina HiSeq-2000 sequencer.

Calculation of copy number of mRNAs

Gene expression levels were calculated by using the reads per kb per million reads (RPKM) method, using the formula shown below:

$$\text{RPKM (A)} = \frac{10^6 C}{\text{NL}/10^3}$$

in which RPKM (A) represents the expression of gene A, C represents the number of reads that are uniquely aligned to gene A, N is the total number of reads that are uniquely aligned to all genes, and L is the number of bases in gene A. The RPKM method is capable of eliminating the influence of differences in gene length and sequencing discrepancies on the calculation of gene expression. Therefore, the calcu-

lated gene expression can be directly used for comparing the difference in gene expression among samples. When more than one transcript exists for a gene, the longest transcript is used to calculate the gene expression level and coverage. Gene coverage is the percentage of a gene covered by reads. This value is equal to the ratio of the base number in a gene covered by unique mapping reads to the total base number of that gene.

Results

OMVs deliver UreA to gastric epithelial cells

A large amount of *H. pylori* urease is released upon bacterial autolysis and binds to the surface of viable *H. pylori* (Dunn *et al.*, 1997). Proteomic analysis has shown that UreA is present in the OMVs secreted from *H. pylori* CCUG 17875 strain (Olofsson *et al.*, 2010). These results suggest that *H. pylori* urease can be secreted from bacteria to extracellular milieu via OMVs. To determine whether *H. pylori* 26695 strain also secreted UreA via OMVs, bacteria were cultured in a thin-layer liquid culture system and OMVs were then purified from the culture supernatant. TEM analysis showed that *H. pylori* 26695 strain produced and secreted spherical nanovesicles (Fig. 1A). SDS-PAGE was performed to verify OMVs. Protein bands of OMVs were different from those of bacterial lysates and outer membrane protein fractions (Fig. 1B). Western blot analysis showed that UreA was present in the OMVs of *H. pylori* 26695 strain (Fig. 1C). Next, to determine whether OMVs played a role in the delivery of UreA to gastric epithelial cells, AGS cells were treated with *H. pylori* OMVs for 4 h and were then stained with a monoclonal anti-UreA antibody, followed by staining with an Alexa 488-conjugated goat anti-mouse IgG antibody. UreA was detected in both the cytoplasm and nuclei of AGS cells (Fig. 2). These results suggest that OMVs are an important vehicle by which the UreA produced by *H. pylori* is delivered to gastric epithelial cells.

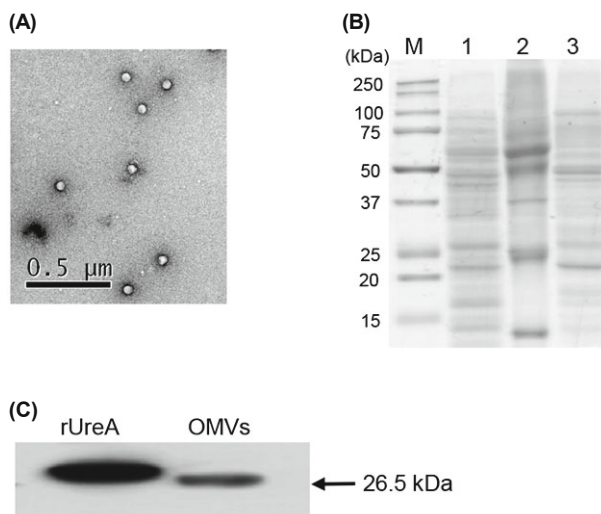


Fig. 1. *H. pylori* OMVs contain UreA. (A) Transmission electron micrograph of OMVs purified from *H. pylori* 26695 strain. (B) Protein profiles of *H. pylori* OMVs. Lanes: M, molecular size markers; 1, bacterial lysates of *H. pylori*; 2, purified OMVs; 3, outer membrane proteins. (C) Identification of UreA in *H. pylori* OMVs. OMV samples were separated by 12% SDS-PAGE and were immunoblotted with a monoclonal anti-UreA antibody. rUreA proteins were used as a positive control.

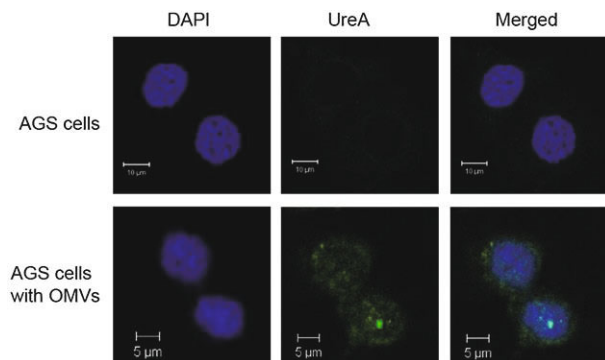


Fig. 2. *H. pylori* OMVs deliver UreA to gastric epithelial cells. AGS cells were treated with *H. pylori* OMVs (a protein concentration of 10 μg/ml) for 4 h. The cells were fixed, permeabilized with Triton X-100, and stained with a monoclonal anti-UreA antibody, followed by staining with an Alexa 488-conjugated goat anti-mouse IgG antibody (green). DAPI was used to stain the nuclei (blue). The distribution of UreA was analyzed by confocal laser microscopy.

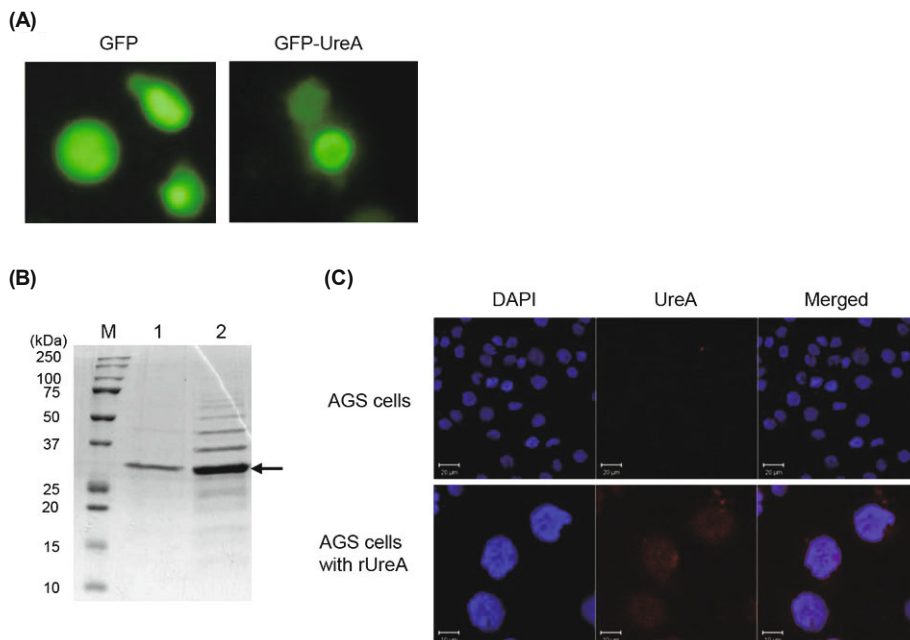


Fig. 3. Nuclear targeting of *H. pylori* UreA in AGS cells. (A) Nuclear localization of *H. pylori* UreA fused with GFP in gastric epithelial cells. AGS cells were transfected with plasmids constructs of *ureA* in the pcDNATM 6.2/N-EmGFP-DEST vector (GFP-UreA) or the empty vector (GFP) and were incubated for 18 h. Subcellular localization of the GFP-tagged UreA proteins was observed by fluorescence microscopy. (B) SDS-PAGE of His-tagged rUreA proteins. The recombinant His-tagged UreA proteins were produced using a Gateway cloning system. Lanes: M, molecular size markers; 1, the purified rUreA proteins; 2, rUreA proteins obtained from bacterial cell lysates. An arrow indicates His-tagged rUreA. (C) Subcellular localization of rUreA in AGS cells. rUreA proteins were directly delivered to AGS cells using a protein transfection system and cells were incubated for 4 h. UreA was labeled with a monoclonal anti-mouse UreA antibody, followed by staining with an Alexa 568-conjugated goat anti-mouse IgG antibody. The nuclei were stained with DAPI. rUreA proteins were distributed in both the cytoplasm and nuclei of AGS cells.

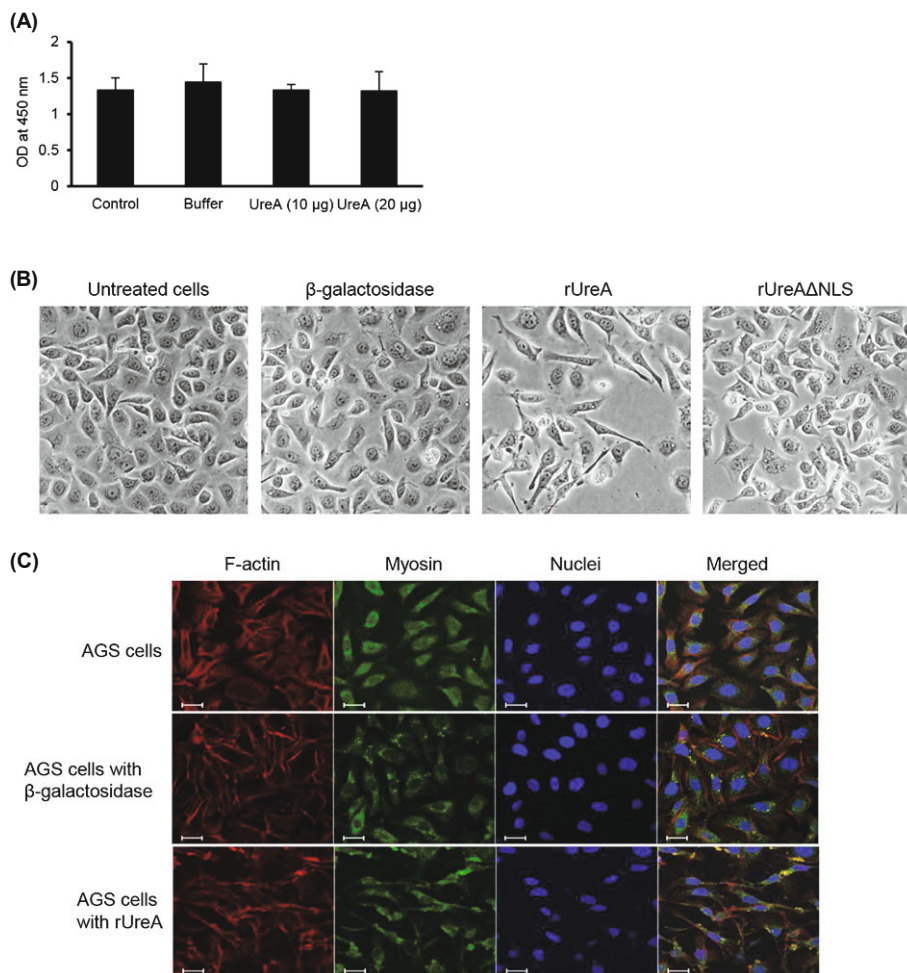


Fig. 4. Morphological changes induced by rUreA proteins in AGS cells. (A) AGS cells were treated with rUreA proteins using a protein transfection system or were treated with the same volume of transfection buffer, and were then incubated for 24 h. Cellular viability was measured using the WST1 assay. (B) rUreA, rUreA Δ NLS, or β -galactosidase (an amount equivalent to a protein concentration of 10 μ g/ml) was delivered directly to AGS cells using a protein transfection system, and cells were then incubated for 24 h. Cellular morphology was observed using a phase-contrast inverted microscope. Magnification, $\times 100$. (C) AGS cells were treated with rUreA proteins (an amount equivalent to a protein concentration of 10 μ g/ml) using a protein transfection system, and were then incubated for 24 h. Cells were fixed, permeabilized with Triton X-100, and stained with Alexa Fluor 568 phalloidin and anti-myosin antibodies, followed by Alexa 488-conjugated goat anti-mouse IgG antibody. The nucleus was stained with DAPI. Cellular morphology was observed using a confocal laser microscope. As a control, AGS cells were treated with 10 μ g/ml of β -galactosidase using a protein transfection system. Scale bar: 20 μ m.

UreA targets the nuclei of gastric epithelial cells

We previously showed that GFP-tagged UreA targeted the nuclei of COS-7 cells via NLSs, whereas GFP-tagged UreA Δ NLS was localized in the cytoplasm of cells (Lee *et al.*, 2012). To determine whether UreA could target the nuclei of effector cells, gastric epithelial AGS cells were transfected with plasmid constructs of *ureA* cloned into the pcDNATM6.2/N-EmGFP-DEST vector, and the subcellular distribution of GFP-tagged UreA was then determined by fluorescence microscopy. Green fluorescence was observed in both the cytoplasm and nuclei of AGS cells, but was predominantly observed in the nuclei (Fig. 3A). To obtain further direct evidence of the nuclear targeting of UreA in AGS cells, rUreA proteins were produced using a Gateway cloning system (Fig. 3B) and directly delivered into AGS cells using a protein transfection system. Similar to the delivery of UreA via OMVs (Fig. 2), confocal microscopy showed that rUreA proteins were detected in both the cytoplasm and nuclei of AGS cells (Fig. 3C). Taken together, our results suggest that *H. pylori* UreA targets the nuclei of gastric epithelial cells after delivery to the host cells via OMVs.

Nuclear targeting of UreA induces morphological changes in AGS cells

To determine whether UreA could induce any cellular change after nuclear targeting, rUreA proteins were delivered directly to AGS cells using a protein transfection system and the cellular viability was determined 24 h after the treatment. Because cytotoxic virulence-associated factors, such as CagA and VacA, were found to be associated with *H. pylori* OMVs and showed the same biological activity that mediated by whole bacteria (Ricci *et al.*, 2005; Olofsson *et al.*, 2010), AGS cells were treated with rUreA proteins, instead of OMVs purified from *H. pylori* 26695 strain. rUreA proteins did not induce cytotoxicity in AGS cells that had been treated with up to 20 μ g/ml (Fig. 4A). However, rUreA proteins (≥ 10 μ g in 50 μ l of buffer) induced morphological changes in AGS cells, such as elongation of the cells (Fig. 4B). As a control, β -galactosidase (10 μ g) was delivered to AGS cells using the protein transfection system and the same volume

(50 μ l) of dialysis buffer as that used for purification of recombinant proteins was treated to the AGS cells. β -Galactosidase and dialysis buffer (data not shown) did not induce any morphological change in AGS cells, as compared to untreated control cells. Furthermore, AGS cells treated with rUreA Δ NLS proteins did not show this morphological change (Fig. 4B), suggesting that nuclear targeting of UreA is a prerequisite for induction of morphological changes in AGS cells. Next, to determine whether morphological changes of AGS cells induced by rUreA proteins were associated with reorganization of actin filaments or myosin, AGS cells were treated with rUreA proteins and stained with Alexa Fluor-568 phalloidin and anti-myosin antibodies. Cellular shrinkage and cytoplasmic elongation were observed in AGS cells treated with rUreA proteins (Fig. 4C). Our results suggested that nuclear targeting of UreA induces morphological changes in AGS cells.

Nuclear targeting of UreA differentially regulates morphogenesis-related genes

In order to investigate whether induction of morphological changes by nuclear targeting of UreA was associated with regulation of morphogenesis-related genes in AGS cells, a genome-wide expression profile in AGS cells in the process of responding to UreA was measured using the NGS technology. Two sets of AGS cells were transfected with plasmid constructs of *ureA* cloned into the destination vector pcDNATM6.2/N-EmGFP-DEST, or with the empty vector. One set of cells was used for a western blotting assay to determine nuclear targeting of GFP-UreA proteins, and the other was used for NGS analysis. The transfection efficiency of AGS cells with both the GFP-tagged UreA clone and the destination vector alone reached approximately 70%, as determined using fluorescence microscopy. In order to determine whether GFP-tagged UreA proteins localized to the nuclei of AGS cells, western blotting analysis was performed using a monoclonal anti-UreA antibody. Intact and degraded GFP-tagged UreA proteins were detected in the nuclear fraction of AGS cells that had been transfected with the plasmid constructs of GFP-tagged UreA clone (Fig. 5). Total RNA was extracted from AGS cells transfected with a plasmid constructs of GFP-tagged UreA clone or the destination vector, and the copy number of mRNA in each gene was calculated. A total of 347 genes were differentially up-regulated by GFP-tagged UreA, with at least a two-fold change, whereas 301 were down-regulated. Among the 648 differentially regulated genes, 102 (15.7%) were found to be associated with cellular morphogenesis; 67 of these were up-regulated by GFP-tagged UreA (Supplementary data Table S1), whereas 35 were down-regulated (Supplementary data Table S2). These results suggest that UreA differentially regulates a wide range of cellular genes, as well as morphogenesis-related genes, which are possibly associated with the induction of morphological changes in AGS cells.

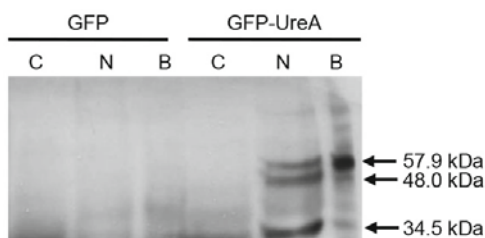


Fig. 5. Nuclear translocation of GFP-tagged UreA proteins in AGS cells. AGS cells were transfected with the destination vector pcDNATM6.2/N-EmGFP-DEST or plasmid constructs of *ureA* in destination vector, and then incubated for 24 h. After harvesting the cells, the nuclear and cytosolic fractions were isolated. The nuclear (N) and cytosolic (C) fractions and bacterial lysates (B) were separated by 12% SDS-PAGE and western blotting was performed using a monoclonal anti-UreA antibody. Intact and degraded GFP-tagged UreA proteins were detected in the nuclear fraction and bacterial lysates.

Discussion

The present study shows that nuclear targeting of *H. pylori* UreA induces morphological changes in gastric epithelial

cells. Besides its main role in the neutralization of gastric acid, *H. pylori* urease may indirectly interfere with host cell biology. Although cellular changes in gastric epithelial cells induced by nuclear targeting of *H. pylori* UreA were demonstrated in AGS cells treated with rUreA, but not with OMVs or whole bacteria, this is the first to report both molecular and morphological changes of host cells induced by nuclear targeting of *H. pylori*-derived molecules.

Delivery of bacterial proteins to the cytoplasm of host cells is a prerequisite for nuclear targeting. We previously showed that *H. pylori* UreA targeted the nuclei of fibroblast COS-7 cells via a functional NLS, ₂₁KKRKEK₂₆, but we did not determine the mechanisms by which UreA delivered to the host cells (Lee *et al.*, 2012). *H. pylori* delivers specific virulence factors, such as CagA, directly to host cells through the type IV secretion system (Naumann and Crabtree, 2004; Lamb *et al.*, 2009). In addition, many virulence-associated factors, including AlpA/B, BabA, OipA, SabA, HopQ, VacA, HtrA, CagA, γ -glutamyl transpeptidase, and UreA, were identified in OMVs from *H. pylori* CCUG 17875 (Olofsson *et al.*, 2010), suggesting that OMVs can deliver these virulence factors to host cells simultaneously. In the present study, we showed that *H. pylori* 26695 strain secreted UreA through OMVs during *in vitro* culture, and that UreA was translocated into gastric epithelial AGS cells via OMVs. Our results suggest that OMVs can deliver bacterial effector proteins, including UreA, to gastric epithelial cells during *H. pylori* infection.

In the present study, we demonstrated that nuclear targeting of rUreA proteins induces the morphological changes in AGS cells. Cellular elongation was also observed in COS-7 cells transfected with the plasmid constructs of *ureA* 24 h after transfection (Lee *et al.*, 2012). Marked changes were observed in actin filaments of AGS cells. However, in our study, rUreA Δ NLS was neither delivered to the nuclei of gastric epithelial cells, nor resulted in morphological changes in AGS cells. This result suggests that morphological changes of AGS cells were only induced by nuclear targeting of UreA. We treated AGS cells with rUreA, but not with *H. pylori* OMVs, because CagA, which can induce a hummingbird phenotype, has been identified on the surface of OMVs (Olofsson *et al.*, 2010). The *H. pylori* oncoprotein, CagA, is known to induce morphological changes in gastric epithelial cells, such as cellular spreading and elongation, that is, the so-called hummingbird phenotype (Yamahashi and Hatakeyama, 2013). Upon delivery into gastric epithelial cells via the type IV secretion system, CagA interacts with SH2 domain-containing protein tyrosine phosphatase 2 (SHP2) and deregulates SHP2 phosphatase activity. CagA-stimulated SHP2 activates the ERK MAP kinase signaling pathway and dephosphorylates focal adhesion kinase (FAK). Both ERK activation and FAK inactivation by CagA-deregulated SHP2 induce the hummingbird phenotype (Higashi *et al.*, 2004; Tsutsumi *et al.*, 2006; Yamahashi and Hatakeyama, 2013). CagA also binds to the kinase catalytic domain of PAR1 (polarity regulating serine/threonine kinase) and inhibits PAR1 kinase activity (Saadat *et al.*, 2007; Yamahashi and Hatakeyama, 2013). CagA causes potentiation of GEF-H1-dependent RhoA activation, which stimulates RhoA-dependent stress fiber formation. As a result, both CagA-SHP2

and CagA-PAR1 interactions not only perturb the microtubule-dependent cytoskeletal system but also deregulate the actin-dependent cytoskeletal system, both of which are involved in induction of the hummingbird phenotype (Yamahashi and Hatakeyama, 2013). A hummingbird phenotype is considered to mimic an epithelial-mesenchymal transition (EMT) (Polyak and Weinberg, 2009; Watanabe *et al.*, 2014). EMT participates in tumor promotion and progression of cancer cells. Expression of epithelial cell markers, such as cytokeratins and E-cadherin, is down-regulated in EMT, whereas mesenchymal proteins, including vimentin, fibronectin, N-cadherin, and integrin, are up-regulated. We did not determine cellular proteins interacting with UreA in the nuclei of host cells and the molecular mechanisms associated with morphological changes in gastric epithelial cells induced by *H. pylori* UreA in this study. Instead, we determined the expression of genes associated with the UreA-induced alteration of host cell morphology. It is of great importance that gene expression was globally regulated in AGS cells that had been transfected with plasmid constructs of GFP-tagged UreA. Among the differentially regulated genes, 102 of the 648 genes that were differentially regulated were associated with cellular morphogenesis. These results suggest that nuclear targeting of UreA induces both molecular changes, such as global regulation of gene expression, and cellular changes, such as the morphological changes, in gastric epithelial cells. The mechanisms regulating morphogenesis-related genes or EMT-associated genes that are induced through nuclear targeting of UreA and the association thereof with morphological changes in gastric epithelial cells should be determined. Another important issue for future research is the detailed role played by UreA in the morphogenetic activity in *H. pylori* infection *in vivo*.

In conclusion, to the best of our knowledge, this is the first report on the alteration of host cell biology that is induced by nuclear targeting of *H. pylori*-derived proteins. UreA displays biological effects that are independent of enzymatic activity, such as morphological changes brought about in gastric epithelial cells through cellular translocation of UreA via OMVs and its subsequent nuclear targeting. Further studies are required to better understand the pathomolecular mechanisms exerted by nuclear targeting of *H. pylori* proteins.

Acknowledgements

This research was supported by the National Research Foundation of Korea (NRF) grant funded by the Korean government (MEST) (2011-0015975).

References

- Backert, S., Clyne, M., and Tegtmeyer, N. 2011. Molecular mechanisms of gastric epithelial cell adhesion and injection of CagA by *Helicobacter pylori*. *Cell. Commun. Signal.* **9**, 28.
- Benabdillah, R., Mota, L.J., Lutzelschwab, S., Demoinet, E., and Cornelis, G.R. 2004. Identification of a nuclear targeting signal in YopM from *Yersinia* spp. *Microb. Pathog.* **36**, 247–261.
- Choi, C.H., Hyun, S.H., Lee, J.Y., Lee, J.S., Lee, Y.S., Kim, S.A., Chae,

- J.P., Yoo, S.M., and Lee, J.C. 2008. *Acinetobacter baumannii* outer membrane protein A targets the nucleus and induces cytotoxicity. *Cell. Microbiol.* **10**, 309–319.
- Cover, T.L. and Blanke, S.R. 2005. *Helicobacter pylori* VacA, a paradigm for toxin multifunctionality. *Nat. Rev. Microbiol.* **3**, 320–332.
- Dunn, B.E., Vakil, N.B., Schneider, B.G., Miller, M.M., Zitzer, J.B., Peutz, T., and Phadnis, S.H. 1997. Localization of *Helicobacter pylori* urease and heat shock protein in human gastric biopsies. *Infect. Immun.* **65**, 1181–1188.
- Eaton, K.A. and Krakowka, S. 1994. Effect of gastric pH on urease-dependent colonization of gnotobiotic piglets by *Helicobacter pylori*. *Infect. Immun.* **62**, 3604–3607.
- Enarsson, K., Brislert, M., Backert, S., and Quiding-Järbrink, M. 2005. *Helicobacter pylori* induces transendothelial migration of activated memory T cells. *Infect. Immun.* **73**, 761–769.
- Ge, R.G., Wang, D.X., Hao, M.C., and Sun, X.S. 2013. Nickel trafficking system responsible for urease maturation in *Helicobacter pylori*. *World J. Gastroenterol.* **19**, 8211–8218.
- Gobert, A.P., Mersey, B.D., Cheng, Y., Blumberg, D.R., Newton, J.C., and Wilson, K.T. 2002. Urease release by *Helicobacter pylori* stimulates macrophage inducible nitric oxide synthase. *J. Immunol.* **168**, 6002–6006.
- Ha, N.C., Oh, S.T., Sung, J.Y., Cha, K.A., Lee, M.H., and Oh, B.H. 2001. Supramolecular assembly and acid resistance of *Helicobacter pylori* urease. *Nat. Struct. Biol.* **8**, 505e9.
- Handa, O., Naito, Y., and Yoshikawa, T. 2007. CagA protein of *Helicobacter pylori*: a hijacker of gastric epithelial cell signaling. *Biochem. Pharmacol.* **73**, 1697–1702.
- Haraga, A. and Miller, S.I. 2003. A *Salmonella enterica* serovar typhimurium translocated leucine-rich repeat effector protein inhibits NF- κ B-dependent gene expression. *Infect. Immun.* **71**, 4052–4058.
- Harris, P.R., Mobley, H.L., Perez-Perez, G.I., Blaser, M.J., and Smith, P.D. 1996. *Helicobacter pylori* urease is a potent stimulus of mononuclear phagocyte activation and inflammatory cytokine production. *Gastroenterology* **111**, 419–425.
- Higashi, H., Nakaya, A., Tsutsumi, R., Yokoyama, K., Fujii, Y., Ishikawa, S., Higuchi, M., Takahashi, A., Kurashima, Y., Teishikata, Y., et al. 2004. *Helicobacter pylori* CagA induces Ras-independent morphogenetic response through SHP-2 recruitment and activation. *J. Biol. Chem.* **279**, 17205–17216.
- Hoy, B., Löwer, M., Weydig, C., Carra, G., Tegtmeyer, N., Geppert, T., Schröder, P., Sewald, N., Backert, S., Schneider, G., et al. 2010. *Helicobacter pylori* HtrA is a new secreted virulence factor that cleaves E-cadherin to disrupt intercellular adhesion. *EMBO Rep.* **11**, 798–804.
- Hu, L.T. and Mobley, H.L. 1990. Purification and N-terminal analysis of urease from *Helicobacter pylori*. *Infect. Immun.* **58**, 992–998.
- Illver, D., Arnqvist, A., Ogren, J., Frick, I.M., Kersulyte, D., Incecik, E.T., Berg, D.E., Covacci, A., Engstrand, L., and Boren, T. 1998. *Helicobacter pylori* adhesin binding fucosylated histo-blood group antigens revealed by retagging. *Science* **279**, 373–377.
- Joo, J.S., Park, K.C., Song, J.Y., Kim, D.H., Lee, K.J., Kwon, Y.C., Kim, J.M., Kim, K.M., Youn, H.S., Kang, H.L., et al. 2010. Thin-layer liquid culture technique for the growth of *Helicobacter pylori*. *Helicobacter* **15**, 295–302.
- Kim, J.I., Baik, S.C., Cho, M.J., Lee, W.K., and Rhee, K.H. 1991. Purification of the urease of *Helicobacter pylori* and production of monoclonal antibody to the urease of *Helicobacter pylori*. *J. Korean Soc. Microbiol.* **26**, 531–540.
- Kim, K.M., Lee, S.G., Park, M.G., Song, J.Y., Kang, H.L., Lee, W.K., Cho, M.J., Rhee, K.H., Youn, H.S., and Baik, S.C. 2007. γ -Glutamyltranspeptidase of *Helicobacter pylori* induces mitochondria-mediated apoptosis in AGS cells. *Biochem. Biophys. Res. Commun.* **355**, 562–567.
- Kwon, S.O., Gho, Y.S., Lee, J.C., and Kim, S.I. 2009. Proteome analysis of outer membrane vesicles from a clinical *Acinetobacter baumannii* isolate. *FEMS Microbiol. Lett.* **297**, 150–156.
- Lamb, A., Yang, X.D., Tsang, Y.H., Li, J.D., Higashi, H., Hatakeyama, M., Peek, R.M., Blanke, S.R., and Chen, L.F. 2009. *Helicobacter pylori* CagA activates NF- κ B by targeting TAK1 for TRAF6-mediated Lys 63 ubiquitination. *EMBO Rep.* **10**, 1242–1249.
- Lange, A., Mills, R.E., Lange, C.J., Stewart, M., Devine, S.E., and Corbett, A.H. 2007. Classical nuclear localization signals: definition, function, and interaction with importin α . *J. Biol. Chem.* **282**, 5101–5105.
- Lee, J.C., Kim, D.S., Moon, D.C., Lee, J.H., Kim, M.J., Lee, S.M., Lee, Y.S., Kang, S.W., Lee, E.J., Kang, S.S., et al. 2009. Prediction of bacterial proteins carrying a nuclear localization signal and nuclear targeting of HsdM from *Klebsiella pneumoniae*. *J. Microbiol.* **47**, 641–645.
- Lee, J.H., Jun, S.H., Baik, S.C., Kim, D.R., Park, J.Y., Lee, Y.S., Choi, C.H., and Lee, J.C. 2012. Prediction and screening of nuclear targeting proteins with nuclear localization signals in *Helicobacter pylori*. *J. Microbiol. Methods* **91**, 490–496.
- Mahdavi, J., Sondén, B., Hurtig, M., Olfat, F.O., Forsberg, L., Roche, N., Angstrom, J., Larsson, T., Teneberg, S., Karlsson, K.A., et al. 2002. *Helicobacter pylori* SabA adhesin in persistent infection and chronic inflammation. *Science* **297**, 573–578.
- Makobongo, M.O., Gilbreath, J.J., and Merrell, D.S. 2014. Nontraditional therapies to treat *Helicobacter pylori* infection. *J. Microbiol.* **52**, 259–272.
- Naumann, M. and Crabtree, J.E. 2004. *Helicobacter pylori*-induced epithelial cell signalling in gastric carcinogenesis. *Trends Microbiol.* **12**, 29–36.
- Odenbreit, S., Faller, G., and Haas, R. 2002. Role of the AlpAB proteins and lipopolysaccharide in adhesion of *Helicobacter pylori* to human gastric tissue. *Int. J. Med. Microbiol.* **292**, 247–256.
- Okuda, J., Toyotome, T., Kataoka, N., Ohno, M., Abe, H., Shimura, Y., Seyedarabi, A., Pickersgill, R., and Sasakawa, C. 2005. *Shigella* effector IpaH9.8 binds to a splicing factor U2AF(35) to modulate host immune responses. *Biochem. Biophys. Res. Commun.* **333**, 531–539.
- Olofsson, A., Vallström, A., Petzold, K., Tegtmeyer, N., Schleucher, J., Carlsson, S., Haas, R., Backert, S., Wai, S.N., Gröbner, G., et al. 2010. Biochemical and functional characterization of *Helicobacter pylori* vesicles. *Mol. Microbiol.* **77**, 1539–1555.
- Pennini, M.E., Perrinet, S., Dautry-Varsat, A., and Subtil, A. 2010. Histone methylation by NUE, a novel nuclear effector of the intracellular pathogen *Chlamydia trachomatis*. *PLoS Pathog.* **6**, e1000995.
- Polyak, K. and Weinberg, R.A. 2009. Transitions between epithelial and mesenchymal states: acquisition of malignant and stem cell traits. *Nat. Rev. Cancer* **9**, 265–273.
- Rassow, J. 2011. *Helicobacter pylori* vacuolating toxin A and apoptosis. *Cell. Commun. Signal* **9**, 26.
- Ricci, V., Chiozzi, V., Necchi, V., Oldani, A., Romano, M., Solcia, E., and Ventura, U. 2005. Free-soluble and outer membrane vesicle-associated VacA from *Helicobacter pylori*: Two forms of release, a different activity. *Biochem. Biophys. Res. Commun.* **337**, 173–178.
- Saadat, I., Higashi, H., Obuse, C., Umeda, M., Murata-Kamiya, N., Saito, Y., Lu, H., Ohnishi, N., Azuma, T., Suzuki, A., et al. 2007. *Helicobacter pylori* CagA targets PAR1/MARK kinase to disrupt epithelial cell polarity. *Nature* **447**, 330–333.
- Seo, L., Jha, B.K., Suh, S.I., Suh, M.H., and Baek W.K. 2014. Microbial profile of the stomach: Comparison between normal mucosa and cancer tissue in the same patient. *J. Bacteriol. Virol.* **44**, 162–169.
- Smiley, R., Bailey, J., Sethuraman, M., Posecion, N., and Showkat, A.M. 2013. Comparative proteomics analysis of sarcosine insoluble outer membrane proteins from clarithromycin resistant

- and sensitive strains of *Helicobacter pylori*. *J. Microbiol.* **51**, 612–618.
- Suerbaum, S. and Michetti, P.** 2002. *Helicobacter pylori* infection. *N. Engl. J. Med.* **347**, 1175–1186.
- Tsutsumi, R., Takahashi, A., Azuma, T., Higashi, H., and Hatakeyama, M.** 2006. Focal adhesion kinase is a substrate and downstream effector of SHP-2 complexed with *Helicobacter pylori* CagA. *Mol. Cell. Biol.* **26**, 261–276.
- Viala, J., Chaput, C., Boneca, I.G., Cardona, A., Girardin, S.E., Moran, A.P., Athman, R., Mémet, S., Huerre, M.R., Coyle, A.J., et al.** 2004. Nod1 responds to peptidoglycan delivered by the *Helicobacter pylori* cag pathogenicity island. *Nat. Immunol.* **5**, 1166–1174.
- Watanabe, T., Takahashi, A., Suzuki, K., Kurusu-Kanno, M., Yamaguchi, K., Fujiki, H., and Suganuma, M.** 2014. Epithelial-mesenchymal transition in human gastric cancer cell lines induced by TNF- α -inducing protein of *Helicobacter pylori*. *Int. J. Cancer* **134**, 2373–2782.
- Wessler, S., Gimona, M., and Rieder, G.** 2011. Regulation of the actin cytoskeleton in *Helicobacter pylori*-induced migration and invasive growth of gastric epithelial cells. *Cell Commun. Signal* **9**, 27.
- Yamashita, Y. and Hatakeyama, M.** 2013. PAR1b takes the stage in the morphogenetic and motogenic activity of *Helicobacter pylori* CagA oncoprotein. *Cell Adh. Migr.* **7**, 11–18.
- Yamaoka, Y., Kwon, D.H., and Graham, D.Y.** 2000. A M(r) 34,000 proinflammatory outer membrane protein (oipA) of *Helicobacter pylori*. *Proc. Natl. Acad. Sci. USA* **97**, 7533–7538.
- Yu, X.W., Xu, Y., Gong, Y.H., Qian, X., and Yuan, Y.** 2011. *Helicobacter pylori* induces malignant transformation of gastric epithelial cells *in vitro*. *APMIS* **119**, 187–197.